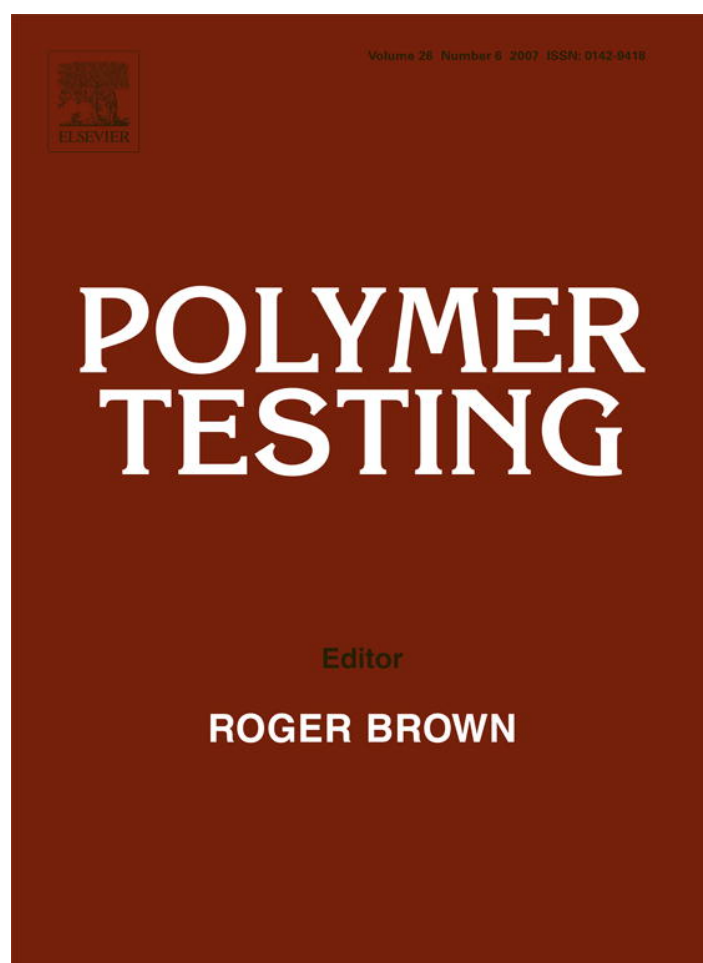


Provided for non-commercial research and education use.  
Not for reproduction, distribution or commercial use.



This article was published in an Elsevier journal. The attached copy is furnished to the author for non-commercial research and education use, including for instruction at the author's institution, sharing with colleagues and providing to institution administration.

Other uses, including reproduction and distribution, or selling or licensing copies, or posting to personal, institutional or third party websites are prohibited.

In most cases authors are permitted to post their version of the article (e.g. in Word or Tex form) to their personal website or institutional repository. Authors requiring further information regarding Elsevier's archiving and manuscript policies are encouraged to visit:

<http://www.elsevier.com/copyright>



## Test Method

# The application of Raman spectroscopy to three-phase characterization of polyethylene crystallinity

W. Lin<sup>\*</sup>, M. Cossar, V. Dang, J. Teh*NOVA Chemicals Research Centre, 2928, 16th Street NE, Calgary, Alta., Canada T2E 7K7*

Received 27 March 2007; accepted 10 May 2007

**Abstract**

The crystallinity of polyethylenes of various densities was studied by applying the Raman spectroscopy technique. Raman spectra were decomposed into the following three components: the orthorhombic crystalline phase, the melt-like amorphous phase and the interfacial phase, which is located between the crystalline and amorphous phases, with possibly highly oriented or ordered chain segments but not in orthorhombic packing. It was found that the amorphous fraction obtained by the Raman method has a small deviation, and it is more reliable to define the crystallinity of polyethylene samples as  $(1 - \text{amorphous fraction}) \times 100\%$  rather than by using the orthorhombic crystalline fraction itself. The calculated results show good linear correlation with the crystallinities derived from other methods - by density, differential scanning calorimetry (DSC), and X-ray diffraction (XRD) measurements.

© 2007 Elsevier Ltd. All rights reserved.

*Keywords:* Raman spectroscopy; Three-phase analysis; Crystallinity; Polyethylene

**1. Introduction**

Crystallinity is an important characteristic of semicrystalline polymers. The commonly used testing methods for determining crystallinity of polyethylene are density, thermal analysis differential scanning calorimetry (DSC), X-ray diffraction (XRD), Raman spectroscopy, nuclear magnetic resonance (NMR), and infrared (IR) spectroscopy. Among these techniques, Raman and NMR are the two methods that will provide direct evidence for the existence of the third, interfacial phase in semicrystalline polymers [1,2].

Strobl and Hagedorn [1] first proposed using Raman spectroscopy to characterize the three-phase morphological structure of semi-crystalline polyethylene. They described semi-crystalline polyethylene as a superposition of three components: an orthorhombic crystalline phase, a melt-like isotropic amorphous phase (random coil molecules), and an anisotropic disordered phase where chains are stretched but lack lateral order. They demonstrated that fractions involved in the three phases could be derived directly from the integrated intensities of characteristic bands without additional calibration. The integrated intensity of the symmetric  $\text{CH}_2$  bending vibration at  $1416\text{ cm}^{-1}$  is used to measure the relative amount of  $\text{CH}_2$  units present in the crystalline phase; the relative amount of the liquid-like amorphous phase can be determined by

<sup>\*</sup>Corresponding author. Tel.: +1 403 250 4700;  
fax: +1 403 250 0621.

E-mail address: [linwen@novachem.com](mailto:linwen@novachem.com) (W. Lin).

deconvoluting the spectrum in the twisting region into a narrow band centered at  $1295\text{ cm}^{-1}$  and a broader component having its maximum intensity at  $1303\text{ cm}^{-1}$ . The total intensity of the  $\text{CH}_2$  twisting region is utilized as an internal standard of intensity because it is independent of the respective amounts of crystalline and amorphous phases. This method was modified and improved by several researchers [3–9], and has been widely accepted and applied in morphological structure analysis of different polyethylenes and their blends.

The original method used by Strobl and Hagedorn [1], as well as that used by Glotin and Mandelkern [3], is a manual decomposition. Later, computer assisted decomposition was adopted to improve the accuracy. Keresztury and Foldes [4] used least-squares curve analysis with a fixed 60% Gaussian and 40% Lorentzian fitting for the Raman spectra of polyethylene. They commented that the manual decomposition method led to overestimated amorphous contents and underestimated interfacial contents. However, Mandelkern and coworkers [5] later declared that the original manual procedure gave the same results as the computer-programmed and curve-fitting methods within small experimental error.

The study of Strobl and Hagedorn using the three-phase analysis on several polyethylene resins found that the crystalline fraction was smaller than that derived from density [1]. Similar results were reported by several researchers [8–11]. Glotin and Mandelkern [3,12] found that the summation of crystalline and interfacial content was identical to the crystallinity derived from density, while Foldes and coworkers [13] contested there was no such relationship between the two methods but just a linear correlation between the crystalline fraction from the Raman spectra analysis and the crystallinity derived from a density test.

For the comparison of crystallinity generated from Raman spectroscopy and the DSC test (enthalpy of fusion), Mandelkern found that the crystallinity level determined from the enthalpy of fusion and the crystalline fraction obtained from the Raman  $1415\text{ cm}^{-1}$  band were in good agreement, while for copolymers and branched samples, the magnitude of DSC results was slightly greater than the Raman crystalline fraction [3,12]. This was confirmed by some other reports [8,13]. However, different results were reported by other researchers [9,11,15–17]. Yan and Jiang [15] found that the DSC crystallinity of oriented HDPE was significantly

higher than the Raman crystalline fraction. The decomposition and curve fitting also have an effect on the results, where Lagaron and coworkers [16] found that the crystalline fraction obtained using  $1295/1303\text{ cm}^{-1}$  bands was closer to the DSC result than that using  $1062/1082\text{ cm}^{-1}$  bands. Perez and coworkers [17] obtained a higher crystalline fraction using the  $1060\text{ cm}^{-1}$  band and a lower crystalline fraction using the  $1416\text{ cm}^{-1}$  band compared to the DSC crystallinity result.

Strobl and Hagedorn obtained coincident values with regard to the fraction of methylene units in the orthorhombic-crystalline phase in Raman spectrum and XRD analysis [1]. While later studies found different results, Perez and coworkers [17] obtained a similar crystalline fraction using the  $1060\text{ cm}^{-1}$  band but a lower one with the  $1416\text{ cm}^{-1}$  band. Experiments conducted by Clas and coworkers [18] and Lagaron and coworkers [14] showed the Raman estimates of crystallinity were lower than those obtained by XRD; while Karacan [11] detected higher Raman crystallinity (including crystalline and interfacial fraction) compared to the X-ray analysis results on gel-spun polyethylene fibers.

Generally, it was recognized that among all the correlations between crystallinities derived from the Raman and other testing techniques, the one with density appeared to give the best correlation [9,18]. This work aims to consolidate the Raman three-phase analysis method and confirm the correlation of Raman crystallinity with other analytical methods applied to polyethylene resins.

## 2. Experimental

### 2.1. Materials

Seventeen polyethylene resins were selected for this study, including two high density polyethylene (HDPE) resins, three single site polyethylene (sPE) resins, one medium density polyethylene (MDPE) resin, five linear low density polyethylene (LLDPE) resins, two low density polyethylene (LDPE) resins, and one plastomer. Their molecular properties are presented in Table 1.

### 2.2. Sample preparation and crystallinity measurements

The polyethylene pellets were compression molded into thin discs of thickness 0.5 mm on a Wabash press following the ASTM D4703 (ISO

Table 1  
Material properties of polyethylene resins

Resin	Density (g/cm <sup>3</sup> )	Melt index (g/10 min)	Comonomer
Plastomer	0.873	5.0	Octene
LLDPE1	0.914	0.9	Octene
sLLDPE	0.918	1.0	Octene
LDPE1	0.919	2.3	None
LDPE2	0.920	0.75	None
LLDPE2	0.920	1.0	Hexene
LLDPE3	0.921	1.0	Butene
LLDPE4	0.922	1.0	Octene
LLDPE5	0.924	0.8	Butene
MDPE	0.935	0.75	Hexene
sMDPE	0.940	5.2	Octene
sHDPE	0.942	1.7	Octene
HDPE1	0.946	8.5 <sup>a</sup>	Hexene
HDPE2	0.954	0.3	Hexene

<sup>a</sup>Measured at 190 °C using 21.6 kg weight.

293) procedure. These plaques were allowed to anneal at room temperature for two weeks prior to any tests.

Density was measured with the density column method ASTM D1505 (ISO 1183-2) at 23 °C. The crystallinity  $\chi_c$  is given by

$$\chi_c = \frac{\rho_c (\rho - \rho_a)}{\rho (\rho_c - \rho_a)}, \quad (1)$$

where  $\rho$  is the density of the semicrystalline polyethylene,  $\rho_a$  is the density of 100% amorphous polyethylene, and  $\rho_c$  is the density of 100% crystalline polyethylene. The values of 0.85 and 1.00 g/cm<sup>3</sup> were selected for the  $\rho_a$  and  $\rho_c$  as commonly reported.

DSC was performed according to ASTM D3418 (ISO 11357-3) on a TA Q1000 DSC. This calorimeter was calibrated with an indium standard. Approximate 5 mg of polymer sample was heated from 0 to 200 °C with a heating rate of 10 °C/min. The endotherm curve was recorded and the degree of crystallinity was evaluated as the ratio between the heat of fusion of the sample and the heat of fusion of the perfect crystalline polyethylene (290 J/g).

XRD was carried out on a SIEMENS GADDS general area detector diffraction system following an internal test procedure. Measurements were performed at room temperature. The X-rays were generated at 40 kV and 40 mA using CuK<sub>α1</sub> radiation (1.541 Å). The detector distance was 6 cm and a 0.5 mm collimator was used. The  $2\theta$ ,  $\omega$  and  $\phi = 0^\circ$

were set for data acquisition. For each diffraction pattern, a total of 10,000,000 counts were collected. The diffraction pattern was then integrated for  $2\theta$  from 4° to 30° and  $\chi$  from -220° to 130°. The crystallinity was obtained for  $2\theta$  range from 8° to 28.5° using commercial software DIFFRACplusProfile.

A Renishaw Confocal Raman Microscope System with a 514.5 nm laser was used to collect the Raman spectra. At least four points determination were carried out on the surface of the plaque from 738 to 1633 cm<sup>-1</sup>. The fraction of CH<sub>2</sub> units in the crystalline orthorhombic phase, or the crystallinity of the sample was calculated using:

$$\alpha_c = \frac{I_{1416}}{0.46I_{ref}}, \quad (2)$$

where the constant 0.46 was taken from Refs. [5,19].

In the CH<sub>2</sub> twisting vibration region, i.e., the region of 1400 and 1250 cm<sup>-1</sup>, a mixed 60% Gaussian and 40% Lorentzian curve-fitting program was used to obtain  $I_{1303}$  in which the two peaks at 1303 and 1295 cm<sup>-1</sup> were fitted. The position of 1303 cm<sup>-1</sup> was limited between 1303 and 1305 cm<sup>-1</sup> region and iterated until being converged. The fraction of amorphous phase was calculated using:

$$\alpha_a = \frac{I_{1303}}{I_{ref}}, \quad (3)$$

where the constant 1.0 was taken from following Refs. [5,19].

Finally, the mass fraction of the interfacial region is given by

$$\alpha_b = 1 - \alpha_c - \alpha_a. \quad (4)$$

### 2.3. Raman spectrum analysis

Two curve fitting procedures were used for spectrum analysis in this study. The curve-fitting technique was performed using Renishaw WiRE 2.0. The first procedure used 100% Gaussian for the three peaks from 1400 to 1550 cm<sup>-1</sup> range, and 60% Gaussian 40% Lorentz for the curve fitting in the range 1250–1400 cm<sup>-1</sup>. The second procedure utilized a single curve fitting process and integration over the whole range from 1220 to 1550 cm<sup>-1</sup>, where the peaks were allowed to float freely for the ratio of Gaussian/Lorentz and automatically optimized by the software for the best fit, with only the amorphous peak position fixed at 1303 cm<sup>-1</sup>.

Since the total integrated intensity  $I_{ref}$  of the  $CH_2$  twisting band at  $1295\text{cm}^{-1}$  is irrelevant to the conformations of molecular chains, it can be used as an internal intensity reference. The total integrated intensity  $I_{ref}$  at  $1295\text{cm}^{-1}$  was measured where the integrated area from  $1352$  to  $1253\text{cm}^{-1}$  was used. The band at  $1416\text{cm}^{-1}$  arises from crystalline regions. A curve fitting program was used to obtain  $I_{1416}$  in which three peaks at  $1461$ ,  $1442$  and  $1416\text{cm}^{-1}$  were fitted in the area between  $1550$  and  $1400\text{cm}^{-1}$  region using a 100% Gaussian distribution and iterated until

convergence. From the integrated intensity of this band ( $I_{1416}$ ), the fraction of  $CH_2$  units in the crystalline orthorhombic phase, or the crystallinity of the sample can be calculated.

### 3. Results and discussions

#### 3.1. Raman three-phase analysis

The crystallinity results obtained by using two different curve fitting methods, i.e. fixed 100%

Table 2  
Three-phases fraction obtained from different analysis methods

Sample	Floating Gaussian/Lorentz fitting (%)			Fixed 100% Gaussian fitting (%)		
	Crystalline	Amorphous	Interphase	Crystalline	Amorphous	Interphase
Plastomer	0.0	82.7	17.3	8.4	85.8	5.7
LLDPE1	25.9	49.4	24.7	43.3	52.2	4.5
sLLDPE	29.3	45.9	24.8	48.1	49.0	2.9
LDPE1	31.0	44.8	24.3	48.3	47.1	4.6
LDPE2	31.1	43.7	25.2	48.6	46.2	5.2
LLDPE2	31.9	44.8	23.3	49.8	47.7	2.5
LLDPE3	32.5	43.1	24.5	50.5	45.7	3.8
LLDPE4	32.4	43.2	24.4	49.9	45.0	4.2
LLDPE5	31.3	42.1	26.6	49.3	44.6	6.3
MDPE	44.9	32.4	22.7	61.8	34.3	3.9
sMDPE	46.8	31.1	22.2	63.6	32.8	3.6
sHDPE	59.9	27.7	12.5	73.8	29.2	-3.0
HDPE1	55.9	25.3	18.8	71.5	26.6	1.9
HDPE2	61.0	19.1	19.9	75.3	19.9	4.8

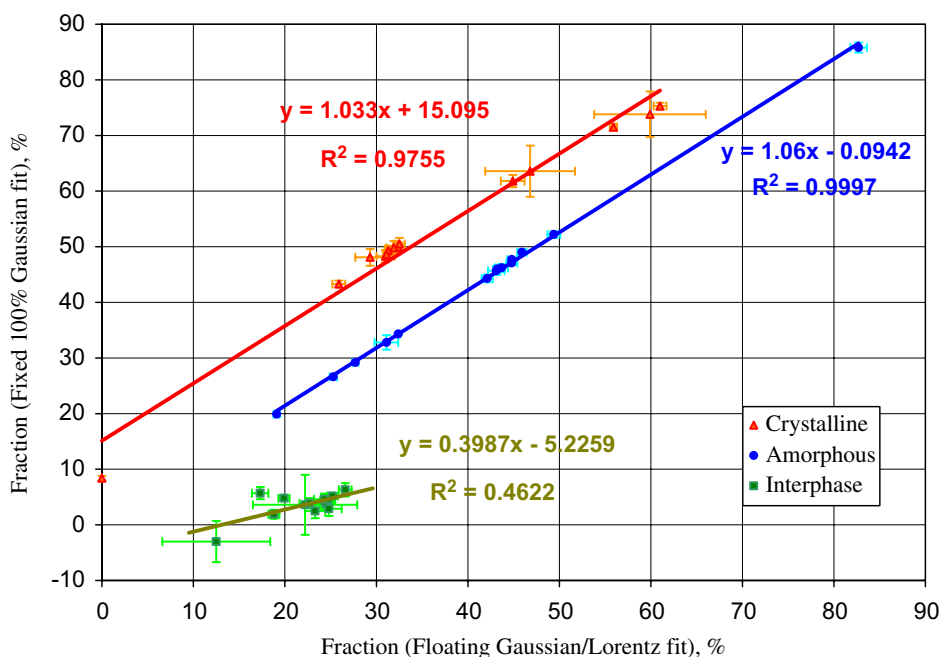


Fig. 1. Three-phase analysis using two cover fitting methods.

Gaussian fit and floating Gaussian/Lorentz fit, are summarized in Table 2 and plotted in Fig. 1 for all three phases. The spread of the results is indicated by the error bars. It can be seen clearly that the amorphous data show less spread for each data point and close to a 'one to one' relation between the two methods of curve fitting. This observation indicates that the measurement of amorphous content of the polyethylene by Raman is a very reproducible and relatively accurate

method. On the other hand, the data for the 'orthorhombic crystalline' fraction show a much larger spread of values for each data point, and a slightly poorer correlation between the two procedures. In addition, the slope is significantly deviated away from unity, and a large intercept can be seen. This large intercept and non unity slope indicate that the two procedures of computing the area of the fit curve are not uniquely defined, or the 'orthorhombic crystalline' fraction may not

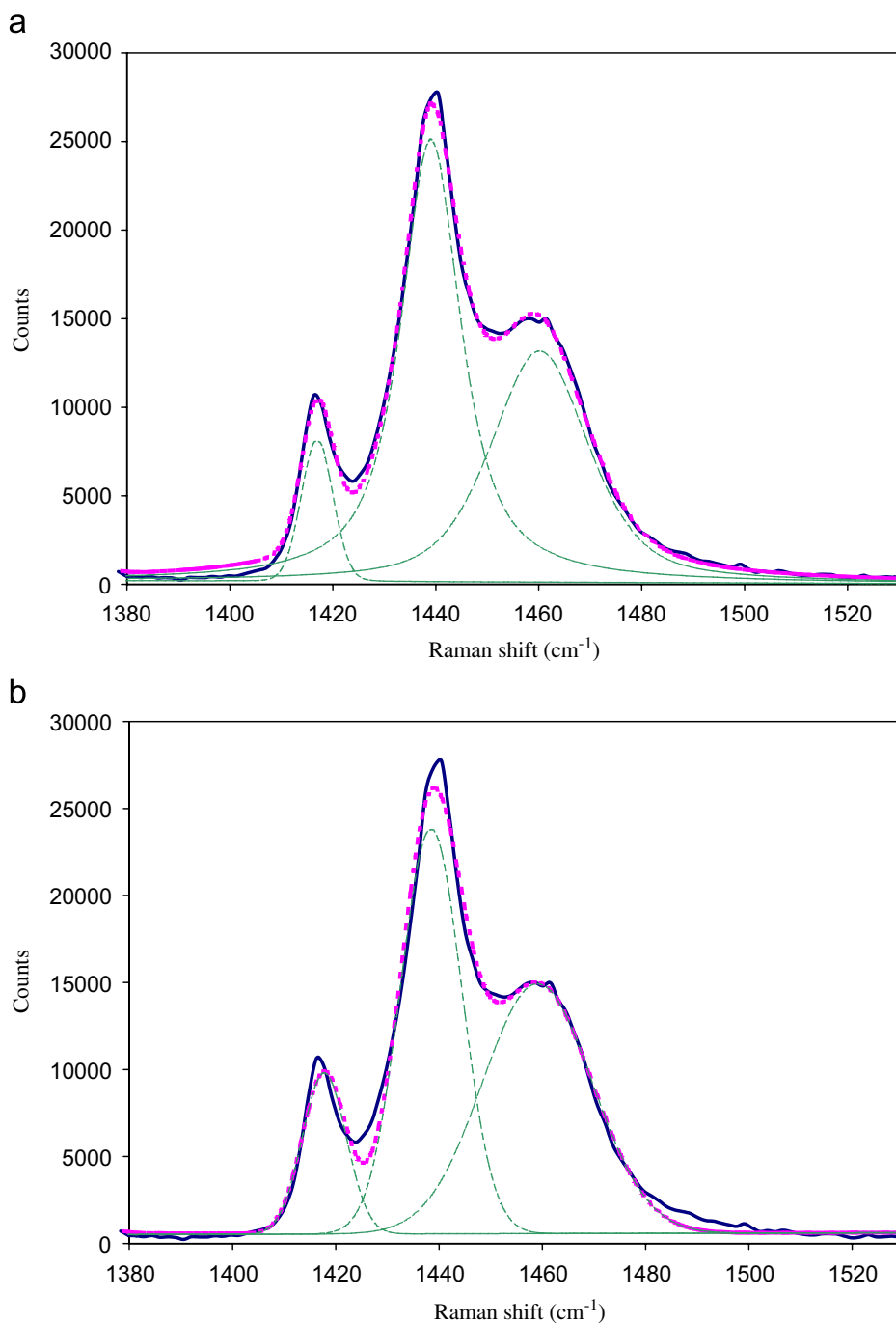


Fig. 2. Comparison of two curve fitting procedures. (a) floating Gaussian/Lorentz fitting; (b) fixed 100% Gaussian fitting.

be uniquely defined by the  $1417\text{cm}^{-1}$  peak as claimed by Strobl and Hagedorn and other researchers. The fixed 100% Gaussian fitting procedure gave a much higher crystalline fraction value, and negative values of interphase were observed on some HDPE samples. In addition, the crystalline fraction of the plastomer could not be detected by the floating Gaussian/Lorentz fit procedure. This indicates that there is no universal equation for the three-phase analysis suitable for all polyethylene resins, the constant may vary, and it will depend on the type of polymer being tested.

Fig. 2 demonstrates the curve fitting of one spectrum with two different procedures: (a) floating Gaussian/Lorentz fitting and (b) fixed 100% Gaussian fitting. Bold solid curves are the original spectra, dash curves are the deconvoluted or decomposed peaks and the bold dot lines are the fitted spectrum. It is obvious that the first procedure (a) gives a better fitting than the fixed 100% Gaussian fitting, as shown by the excellent overlap from visual observation. Therefore, the floating Gaussian/Lorentz fitting method was used in the Raman spectrum three-phase analysis in this study.

### 3.2. Correlation between crystallinities obtained from Raman spectroscopy and other techniques

The Raman three-phase analysis results, as well as the crystallinities derived from the density test, the DSC test and the XRD test are summarized in Table 3. It can be clearly observed that the

Raman crystalline fraction is smaller than the crystallinity obtained by other testing methods, except for some of the XRD that gave lower crystallinity for MDPE and HDPE resins. When the crystallinity is taken as the total of the Raman orthorhombic crystalline and interphase fractions, it will be higher compared to crystallinities derived from other testing techniques. Fig. 3 is the plot of crystallinities obtained from different testing methods as a function of the resin density. Compared to the Raman crystalline fraction itself, the summation of crystalline and interphase fractions has better correlation with the density. Since the amorphous fraction result has very small variations, it is better to use  $(1 - \text{amorphous fraction}) \times 100\%$  as the crystallinity. Table 4 shows the correlation of different testing methods for the determination of the polyethylene crystallinity. The Raman orthorhombic crystalline fraction had a poor correlation ( $R^2 < 0.8$ ) with all the other testing methods; the summation of crystalline and interphase fractions, on the other hand, shows a very good linear correlation ( $R^2 > 0.98$ ) with other techniques. From the Raman study it appears that the crystallinities measured by DSC, X-ray, and density reflect the sum of 100% perfect crystalline fraction (Raman orthorhombic) and some semi-crystalline fraction (Raman interfacial).

The interfacial phase, as measured by the Raman technique, has been demonstrated to be correlated with the tie chains in a recent study on the single site catalyst dual reactor technology in polyethylene rotomolding resin [20].

Table 3  
Crystallinity (%) obtained from different testing methods

Sample	Raman crystalline fraction	Raman $(1 - \text{amorphous}) \times 100\%$	Density crystallinity	DSC crystallinity	XRD crystallinity
Plastomer	0.0	17.3	18.2	8.1	9.6
LLDPE1	25.9	50.6	45.7	42.5	32.7
sLLDPE	29.3	54.1	48.6	44.8	34.7
LDPE1	31.0	55.2	49.3	44.4	34.4
LDPE2	31.1	56.3	49.9	45.5	35.2
LLDPE2	31.9	55.2	49.9	48.4	35.9
LLDPE3	32.5	56.9	50.3	47.1	35.9
LLDPE4	32.4	56.8	51.0	48.9	36.5
LLDPE5	31.3	57.9	52.6	48.5	36.2
MDPE	44.9	67.6	60.2	60.9	43.6
sMDPE	46.8	68.9	63.2	65.2	45.6
sHDPE	59.9	72.3	64.8	67.5	45.7
HDPE1	55.9	74.7	66.8	68.0	46.7
HDPE2	61.0	80.9	72.5	75.6	53.3

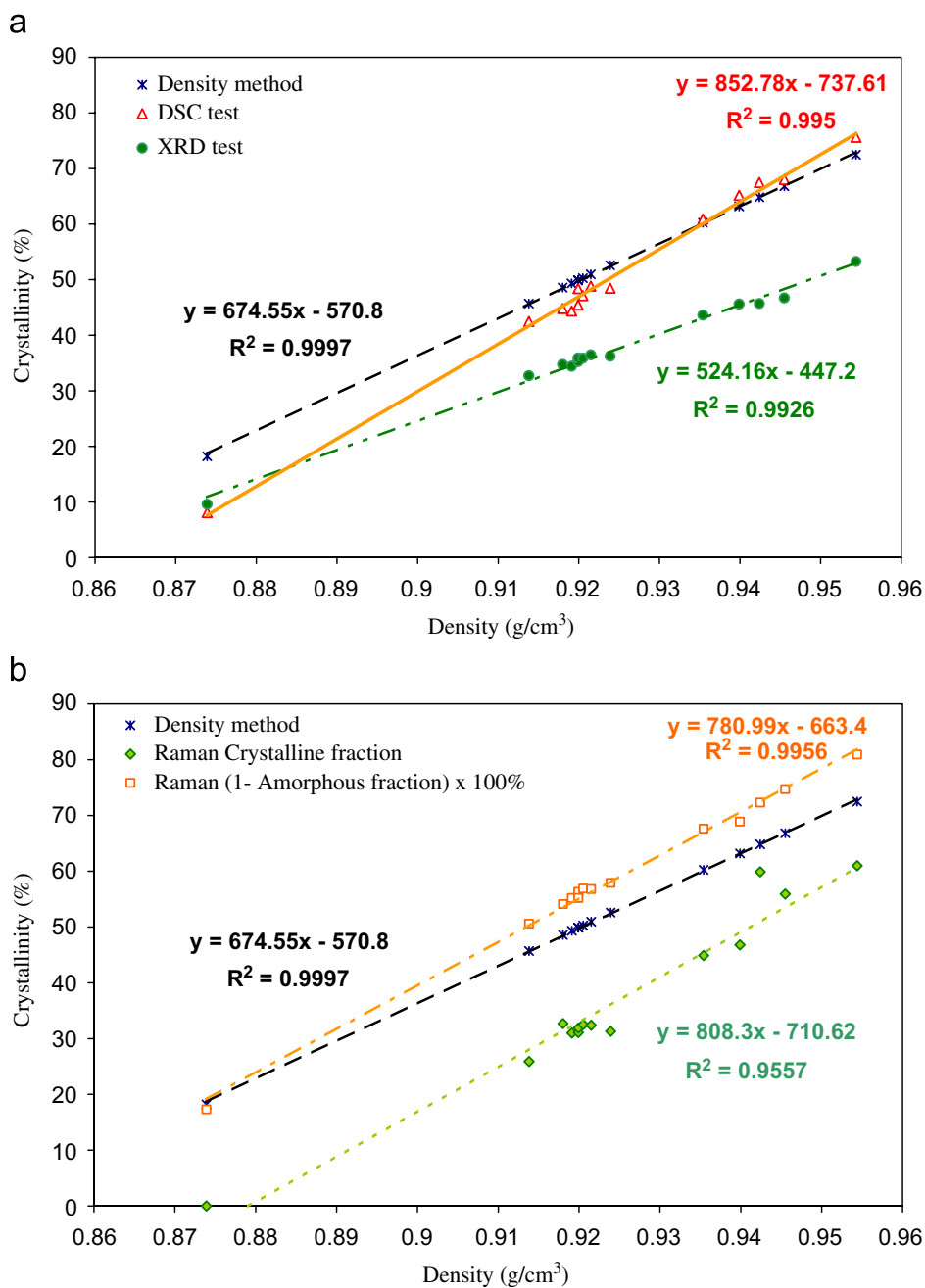


Fig. 3. Crystallinity of different testing methods corresponds to resin density. (a) DSC test and XRD test; (b) Raman crystalline fraction and Raman (1 – amorphous fraction) × 100%.

#### 4. Conclusions

In this work, we have compared the Raman three-phase analysis methods for polyethylene resins covering a broad density range. The fixed 100% Gaussian fitting procedure gives a high crystalline fraction and may result in a negative value on the interphase for HDPE samples; the floating Gaussian/Lorentz fitting procedure yields better fit on the Raman spectrum. However, it cannot detect or

resolve the crystalline fraction of very low density samples (i.e. plastomer).

The crystalline fraction itself has large variations and poor correlation with other crystallinity characterizing techniques such as density measurement, DSC and XRD. The amorphous fraction obtained from Raman three-phase analysis has very good reproducibility. It was further confirmed that the summation of orthorhombic crystalline and interphase fractions as the total crystallinity has good

Table 4  
Correlation of crystallinity with different testing methods

	Density	DSC	XRD	Raman crystalline fraction	Raman (1 – amorphous fraction) × 100%
Density	1	$y = 0.787x + 12.863$ $R^2 = 0.994$	$y = 1.278x + 5.028$ $R^2 = 0.994$	$y = 1.506x + 23.641$ $R^2 = 0.772$	$y = 0.860x + 2.364$ $R^2 = 0.997$
DSC	$y = 1.264x - 15.969$ $R^2 = 0.994$	1	$y = 1.617x - 9.682$ $R^2 = 0.991$	$y = 1.908x + 13.805$ $R^2 = 0.772$	$y = 1.086x - 12.860$ $R^2 = 0.988$
XRD	$y = 0.777x - 3.678$ $R^2 = 0.994$	$y = 0.612x + 6.288$ $R^2 = 0.991$	1	$y = 1.191x + 14.302$ $R^2 = 0.794$	$y = 0.670x - 1.894$ $R^2 = 0.994$
Raman crystalline fraction	$y = 0.513x - 7.669$ $R^2 = 0.772$	$y = 0.405x - 1.128$ $R^2 = 0.772$	$y = 0.667x - 5.520$ $R^2 = 0.794$	1	$y = 0.445x - 6.666$ $R^2 = 0.782$
Raman (1 – amorphous fraction) × 100%	$y = 1.158x - 2.568$ $R^2 = 0.997$	$y = 0.910x + 12.422$ $R^2 = 0.988$	$y = 1.483x + 3.180$ $R^2 = 0.994$	$y = 1.758x + 24.544$ $R^2 = 0.782$	1

correlations with crystallinities determined by other analytical methods. Using this summation as the Raman crystallinity is more reliable and accurate.

### Acknowledgments

The authors would like to thank NOVA Chemicals Corporation for permission to publish this work. The authors are also indebted to their colleagues in the Analytical and Physical Testing Laboratories at NOVA Chemicals for their assistance in establishing the data presented.

### References

- [1] R.G. Strobl, W. Hagedorn, *J. Polym. Sci. Polym. Phys. Ed.* 16 (1978) 1181.
- [2] K. Bergmann, K. Nawotki, *Colloid Polym. Sci.* 219 (1967) 132.
- [3] M. Glotin, L. Mandelkern, *Colloid Polym. Sci.* 260 (1982) 182.
- [4] G. Keresztury, E. Földes, *Polym. Test.* 9 (1990) 329.
- [5] M. Failla, R.G. Alamo, L. Mandelkern, *Polym. Test.* 11 (1992) 151.
- [6] C.C. Naylor, R.J. Meier, B.T. Kip, K.P.J. Williams, S.M. Mason, N. Conroy, D.L. Gerrard, *Macromolecules* 28 (1995) 2969.
- [7] E. Pérez, R. Benavente, R. Quijada, A. Narváez, G.B. Galland, *J. Polym. Sci. Part B Polym. Phys.* 38 (2000) 1440.
- [8] F. Rull, A.C. Prieto, J.M. Casado, F. Sobron, H.G.M. Edwards, *J. Raman Spectrosc.* 24 (1993) 545.
- [9] K.P.J. Williams, N.J. Everall, *J. Raman Spectrosc.* 26 (1995) 427.
- [10] S.D. Clas, R.D. Heyding, D.C. McFaddin, K.E. Russell, M.V. Scammell-Bullock, E.C. Kelusky, D. St-Cyr, *J. Polym. Sci. Part B Polym. Phys.* 26 (1988) 1271.
- [11] I. Karacan, *J. Appl. Polym. Sci.* 101 (2006) 1317.
- [12] L. Mandelkern, *Polym. J.* 17 (1985) 337.
- [13] E. Foldes, G. Keresztury, M. Iring, F. Tudos, *Angew. Makromol. Chem.* 187 (1991) 87.
- [14] J.M. Lagarón, S. López-Quintana, J.C. Rodríguez-Cabello, J.C. Merino, J.M. Pastor, *Polymer* 41 (2000) 2999.
- [15] R. Yan, B. Jiang, *Chin. J. Polym. Sci.* 11 (1993) 76.
- [16] J.C. Rodríguez-Cabello, J. Martín-Monge, J.M. Lagarón, J.M. Pastor, *Macromol. Chem. Phys.* 199 (1998) 2767.
- [17] E. Pérez, R. Benavente, R. Quijada, A. Narváez, G.B. Galland, *J. Polym. Sci. Part B: Polym. Phys.* 38 (2000) 1440.
- [18] S.D. Clas, R.D. Heyding, D.C. McFaddin, K.E. Russell, M.V. Scammell-Bullock, E.C. Kelusky, D. St-Cyr, *J. Polym. Sci. Part B Polym. Phys.* 26 (1988) 1271.
- [19] R.P. Paradkar, S.S. Sakhalkar, X. He, M.S. Ellison, *J. Appl. Polym. Sci.* 88 (2003) 545.
- [20] X. Wang, M. Weber, H. Hay, M. Cossar, *SPE ANTEC*, 2005.